Inorg. Chem. **2004**, *43*, 4056–4063

Metal–Metal Bonded Homo- and Heterobimetallic Compounds of Pt(I) and Pd(I) Supported by a Bridging-*N*,*P*:*N*′,*P*′ Moiety of a Potentially Hexadentate Ligand

Nathan D. Jones,[†] S. Jo Ling Foo, Brian O. Patrick, and Brian R. James*

Department of Chemistry, The University of British Columbia, Vancouver, British Columbia, Canada V6T 1Z1

Received February 9, 2004

Reactions of metal–metal bonded homobimetallic (Pd_2) and heterobimetallic (PtPd) complexes, supported by a *P*,*P*′-bridging-bis(*P*,*N*-chelating) coordination mode of the potentially hexadentate ligand 1,1-bis[di(*o*-*N*,*N*-dimethylanilinyl)phosphino]methane (dmapm), with CO, diethylacetylenedicarboxylate (DEAD), and thiols (RSH) in CH_2Cl_2 are described. At room temperature, *rac*-Pd_2Cl_2(μ-*N*,*P*:*P*′,*N*′-dmapm) gives the stable complexes Pd_2Cl_2(μ-CO)$_2$-(μ-*P*:*P*′-dmapm) and PdCl(η^2-DEAD)(μ-*P*:*P*′,*N*-dmapm)PdCl (which is fluxional in solution), while *rac*-$PtPdCl_2$(μ-*N*,*P*:*P*′,*N*′-dmapm) disproportionates to $PtCl_2$(*P*,*P*′-dmapm) and Pd metal, although at low temperature intermediate carbonyl species are detected in the CO reaction. The reactions with thiols in the presence of triflic acid (HOTf) generate *rac*-[$MPdCl_2$(μ-SR)(μ-*N*,P:*P*′,*N*′-dmapm)][OTf] and H_2 for both M = Pt and Pd. In CH_2Cl_2, PdX_2(dmapm) species (X = halide or CN) exist as equilibrium mixtures of *P*,*P*′- and *P*,*N*-ligated forms. For X = Cl, the *P*,*P*′-*P*,*N* equilibrium is governed by $\Delta H^\circ = -5.5 \pm 0.5$ kJ mol^{-1} and $\Delta S^\circ = 10 \pm 1$ J mol^{-1} K^{-1}, and the ring-strain energy within the *P*,*P*′-isomer is $\sim$32 kJ mol^{-1}; the equilibrium increasingly favors the *P*,*N*-form with X = CN $\gg$ I > Br > Cl. The solid-state structures of *rac*-[$PtPdCl_2$(μ-SEt)(μ-*N*,P:*P*′,*N*′-dmapm)][OTf] and $PdCl_2$(*P*,*N*-dmapm) are presented; the latter contains both bound and free N- and P-atoms of identical types in the same molecule and permits an assessment of σ- and π-bonding between these atoms and Pd.

Introduction

In a search for bimetallic complexes in which both metals act cooperatively during a catalytic cycle,[1] the choice of bridging ligand remains crucial. Tsukada et al.[2] have recently pointed out that Pd_2,[3,4] Pt_2,[5−7] and Pt−Pd[8−10] complexes bridged by two diphosphine (PP) or 2-pyridylphosphine (PN) ligands have rarely been used in catalysis,[11−14] even though their stoichiometric chemistry continues to expand.[15,16] The dearth of catalytic applications has been attributed[2] to the geometries of the complexes that typically forbid the cis juxtaposition of incoming ligands (L in Chart 1A), which is generally essential for elementary catalytic steps.

We note, however, that chair-shaped Pt_2 complexes bridged by two *cis*-P−P ligands do exist and these can accommodate cis L ligands,[17−19] and also that elevated

* To whom correspondence should be addressed. E-mail: brj@chem.ubc.ca.

[†] Current address: Department of Chemistry, University of Alberta, Edmonton, Alberta, Canada T6G 2G2.

(1) Rowlands, G. *Tetrahedron* **2001**, *57*, 1865.
(2) Tsukada, N.; Tamura, O.; Inoue, Y. *Organometallics* **2002**, *21*, 2521.
(3) Pamplin, C. B.; Rettig, S. J.; Patrick, B. O.; James, B. R. *Inorg. Chem.* **2003**, *42*, 4117.
(4) Stockland, R. A.; Anderson, G. K.; Rath, N. P. *J. Am. Chem. Soc.* **1999**, *121*, 7945.
(5) Janka, M.; Anderson, G. K.; Rath, N. P. *Organometallics* **2000**, *19*, 5071.
(6) Irwin, M. J.; Gia, G.; Vittal, J. J.; Puddephatt, R. J. *Organometallics* **1996**, *15*, 5321.
(7) Toronto, D. V.; Balch, A. L. *Inorg. Chem.* **1994**, *33*, 6132.
(8) Xu, C.; Anderson, G. K. *Organometallics* **1996**, *15*, 1760.
(9) Xu, C.; Anderson, G. K. *Organometallics* **1994**, *13*, 3981.
(10) Fallis, K. A.; Xu, C.; Anderson, G. K. *Organometallics* **1993**, *12*, 2243.
(11) Ishii, H.; Goyal, M.; Ueda, M.; Takeuchi, K.; Asai, M. *J. Mol. Catal. A: Chem.* **1999**, *148*, 289.
(12) Ishii, H.; Ueda, M.; Takeuchi, K.; Asai, M. *J. Mol. Catal. A: Chem.* **1999**, *144*, 477.
(13) Wong, T. Y. H.; Barnabas, A. F.; Sallin, D.; James, B. R. *Inorg. Chem.* **1995**, *34*, 2278.
(14) Wong, T. Y. H.; James, B. R.; Wong, P. C.; Mitchell, K. A. R. *J. Mol. Catal. A: Chem.* **1999**, *139*, 159.
(15) Chaudret, B.; Delavaux, B.; Poilblanc, R. *Coord. Chem. Rev.* **1988**, *86*, 191.
(16) Puddephatt, R. J. *Chem. Soc. Rev.* **1983**, *12*, 99.
(17) Azam, K. A.; Ferguson, G.; Ling, S. S. M.; Parvez, M.; Puddephatt, R. J.; Srokowski, D. *Inorg. Chem.* **1985**, *24*, 2799.
(18) Manojlovic-Muir, L.; Muir, K. W.; Frew, A. A.; Ling, S. S. M.; Thomson, M. A.; Puddephatt, R. J. *Organometallics* **1984**, *3*, 1637.

10.1021/ic040019t CCC: $27.50 © 2004 American Chemical Society
Published on Web 05/21/2004

Chart 1. Typical Structures of Bimetallic Complexes Supported by Bridging-Bidentate and by Bridging-Chelating Tetradentate Ligands[a]

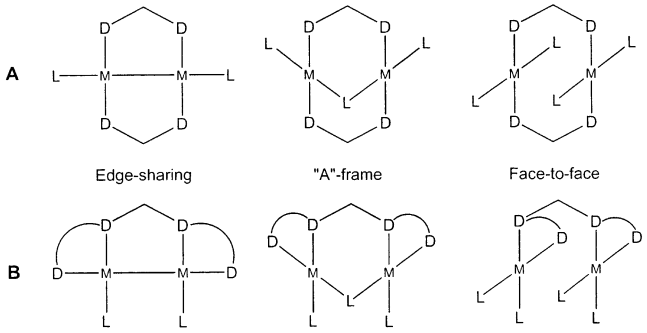

[a] D = donor atom (typically P or N), L = other ligand, M = metal (typically Pt or Pd); adapted from ref 2.

Chart 2. Structural Diagrams of dmapm and $MPdCl_4(\mu\text{-}N,P\text{:}P',N'\text{-dmapm})$ Complexes (M = Pt, Pd)

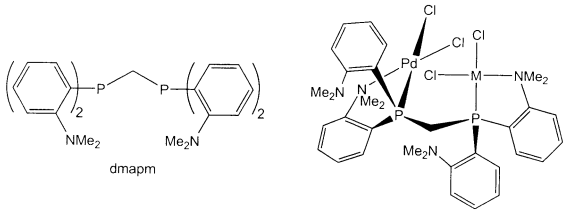

temperatures can invert "A"-frame complexes (Chart 1A) via transition structures with mutually cis (i.e., "W"-like) orientations of the three L ligands.[4] Nevertheless, edge-sharing "A"-frame and face-to-face complexes that permit naturally a cis orientation of L ligands and/or vacant sites should favor catalytic activity. Thus, tetradentate ligands that may form simultaneously both bridges and chelates are attractive scaffolds for bimetallic "cooperative" catalysts, (Chart 1B) and indeed, effective Rh_2 hydroformylation catalysts, based on such a (tetraphosphine) ligand, have been developed by Stanley's group.[20]

Our group has recently reported some diphosphine ligands that bear two *o*-*N*,*N*-dimethylanilinyl groups on each P-atom.[21] One of these, 1,1-bis[di(*o*-*N*,*N*-dimethylanilinyl)-phosphino]methane (dmapm), illustrated in Chart 2, shows a tendency both to bridge metals, given that the P donors are separated by a single CH_2 group, and to form five-membered *P*,*N*-chelate rings [note that *P*,*N*-coordination of dmapm induces chirality at the P-atom]. The only other ligand that spans two metals in this way is the bis(2-pyridylphosphine), $py(Ph)PCH_2P(Ph)py$, reported by Budzelaar et al.[22] We have made face-to-face Pt^{II}_2 complexes containing two *P*,*P*′-chelating-bis(*P*,*N*-bridging), $py_2P(CH_2)_2$-Ppy_2 ligands,[23] and Pd^{II}_2 and Pt^{II}_2 complexes supported by tetradentate ligands that form an *N*,*N*′-bridge and two *N*,*P*-chelate rings are also known.[2,24]

Scheme 1. Bimetallic dmapm Complexes and Their Reaction with Thiols[a]

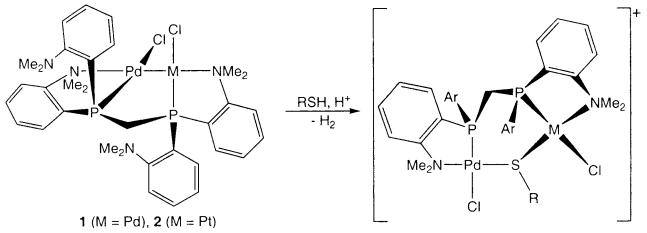

[a] Ar = o-$C_6H_4NMe_2$. For M = Pt, products are *rac*-**10** (R = Et) and *rac*-**11** (R = ^{n}Pr). See text.

We have reported on the synthesis of the metal−metal bonded Pd^{I}_2 complex, *rac*-$Pd_2Cl_2(\mu\text{-}N,P\text{:}P',N'\text{-dmapm})$[25] (**1**, Scheme 1), and the non-metal−metal bonded $M^{II}Pd^{II}$ species $MPdCl_4(\mu\text{-}N,P\text{:}P',N'\text{-dmapm})$[26] (M = Pd, Pt; Chart 2), the last two complexes being effective catalyst precursors for aerobic, aqueous Heck reactions, but not via intermetallic cooperative pathways.[26] Further, we have noted that **1**, unlike $Pd_2Cl_2(\mu\text{-}P\text{:}P'\text{-dppm})_2$ (dppm = $Ph_2PCH_2PPh_2$), reacts with thiols (RSH), in the presence or absence of added acid, to give the bridged-thiolate complex cations, *rac*-$[Pd_2Cl_2(\mu\text{-SR})(\mu\text{-}N,P\text{:}P',N'\text{-dmapm})]^+$, and H_2, via a novel oxidative addition of RS−H across a phosphine-bridged Pd^{I}−Pd^{I} bond (Scheme 1).[25] We are not aware of other reports describing reactions of small molecules with metal−metal bonded complexes supported by tetradentate ligands. In this article, we describe reactions of **1** and its heterobimetallic analogue, *rac*-$PtPdCl_2(\mu\text{-}N,P\text{:}P',N'\text{-dmapm})$ (**2**, Scheme 1), with CO and with diethylacetylenedicarboxylate (DEAD), and the reaction of **2** with RSH (R = Et, ^{n}Pr) in the presence of triflic acid (HOTf). We show that indeed the architecture afforded by the potentially hexadentate, but functionally tetradentate, dmapm ligand gives rise to stoichiometric reaction pathways that are different from those undergone by the analogous bis(P−P)- and bis(P−N)-bridged complexes in the same reactions. In addition, we demonstrate that the incorporation of hemilabile N-donors can give rise to dynamic coordination modes, previously unknown within phosphine-bridged Pd and Pt bimetallic chemistry. The solid-state structure and solution fluxional behavior of PdX_2-(dmapm) (X = Cl (**3**), Br (**4**), I (**5**) and CN (**6**)), are also described; **3** is used in the synthesis of **1**.

Experimental Section

General. Unless otherwise noted, synthetic procedures were performed at room temperature (rt, ~20 °C) using standard Schlenk techniques under an atmosphere of dry Ar or N_2. The dmapm ligand,[21] $PtCl_2(cod)$,[27] *trans*-$PdCl_2(PhCN)_2$,[28] and **1**[25] were made according to literature procedures. Other reagents were purchased from commercial sources and used as supplied. Solvents were dried

(19) Radecka-Paryzek, W.; McLennan, A. J.; Puddephatt, R. J. *Inorg. Chem.* **1986**, *25*, 3097.
(20) (a) Broussard, M. E.; Juma, B.; Train, S. G.; Peng, W.-J.; Laneman, S. A.; Stanley, G. G. *Science* **1993**, *260*, 1784. (b) Aubry, D. A.; Bridges, N. N.; Ezell, K.; Stanley, G. G. *J. Am. Chem. Soc.* **2003**, *125*, 11180.
(21) Jones, N. D.; Meessen, P.; Smith, M. B.; Losehand, U.; Rettig, S. J.; James, B. R. *Can. J. Chem.* **2002**, *80*, 1600.
(22) Budzelaar, P. H. M.; Frijns, J. H. G.; Orpen, A. G. *Organometallics* **1990**, *9*, 1222.
(23) Jones, N. D.; Rettig, S. J.; James, B. R. *J. Cluster Sci.* **1998**, *9*, 243.
(24) Ligtenbarg, A. G.; van der Beukin, E. K.; Veldman, A. M.; Smeets, W. J. J.; Spek, A. L.; Feringa, B. L. *J. Chem. Soc., Dalton Trans.* **1998**, 263.
(25) Foo, S. J. L.; Jones, N. D.; Patrick, B. O.; James, B. R. *Chem. Commun.* **2003**, 988.
(26) Jones, N. D.; James, B. R. *Adv. Synth. Catal.* **2002**, *344*, 1126.
(27) McDermott, J. X.; White, J. F.; Whitesides, G. M. *J. Am. Chem. Soc.* **1976**, *98*, 6521.
(28) Hartley, F. R. *J. Organomet. Chem. Rev., Sect. A* **1970**, *6*, 119.

over the appropriate agents and distilled under N_2 prior to use. NMR spectra were recorded in $CDCl_3$ solution on Varian AV300 (121 MHz for ^{31}P, 282 MHz for ^{19}F) or AV400 (162 MHz for ^{31}P) spectrometers at 300 K, unless otherwise specified. Residual solvent proton (^1H, relative to external $SiMe_4$ δ 0.00) and external $P(OMe)_3$ ($^{31}P\{^1H\}$, δ 141.00 vs external 85% aq H_3PO_4) were used as references; s = singlet, d = doublet, t = triplet, m = multiplet, br = broad, p = pseudo. All *J*-values are given in Hertz. UV−vis spectra were recorded on a Hewlett-Packard 8452A diode array spectrophotometer and are reported as λ_{max} (±2 nm) [ϵ (M^{-1} cm^{-1})]. Conductivity measurements at 25 °C (reported as Λ_M in Ω^{-1} mol^{-1} cm^2) were obtained on 1 mM solutions of the complexes using a Thomas Serfass conductance bridge model RCM151B1 (Arthur H. Thomas Co. Ltd.) connected to a 3404 cell (Yellow Springs Instrument Co.). Mass spectra were measured in LSIMS mode (Kratos Concept IIHQ instrument) with 3-nitrobenzyl alcohol as matrix and are reported as *m*/*z* peaks. Elemental analyses were done in the department here by Mr. P. Borda using a Carlo Erba 1108 analyzer.

Syntheses. *rac*-PtPdCl$_2$(μ-*N*,*P*:*N*′,*P*′-dmapm)·H$_2$O, 2·H$_2$O. To *trans*-$PdCl_2(PhCN)_2$ (130 mg, 0.33 mmol) and dmapm (190 mg, 0.33 mmol) in a Schlenk tube was added CH_2Cl_2 (7 mL). The initially orange solution rapidly turned yellow. The solvent was removed, and EtOH (10 mL) was added, followed by an aqueous solution (5 mL) containing K_2PtCl_4 (140 mg, 0.33 mmol). The orange slurry was heated to 70 °C for 1 h when it turned yellow. An ethanolic solution containing KOH (13 mL, 70 mmol L^{-1}) was added over 3 min and the resulting brown solution stirred at 70 °C for an additional 0.5 h. The solvents were then removed in vacuo, the residue, dried overnight, was partially dissolved in warm C_6H_6 (30 mL), and then the mixture was filtered through a plug of Celite 545 and $MgSO_4$. The brown filtrate was shown by NMR spectroscopy to contain unreacted PtPdCl$_4$(μ-*N*,*P*:*P*′,*N*′-dmapm), formed in situ,[26] and **2**. The Celite-trapped solid was then eluted with CH_2Cl_2 (10 mL), and the brown-red filtrate was concentrated to ~1 mL. Addition of Et_2O (25 mL) gave the green-brown product that was isolated by filtration, washed with Et_2O (3 × 3 mL), and dried in vacuo. Yield: 99 mg (32%). Anal. Calcd for $C_{33}H_{44}N_4Cl_2OP_2PdPt$: C, 41.9; H, 4.7; N, 5.9. Found: C, 41.5; H, 4.6; N, 5.7. ^1H NMR: δ 2.36 (s, 6H, NCH_3), 2.45 (s, 6H, NCH_3), 2.78 (s, 3H, NCH_3), 3.02 (s, 3H, NCH_3), 3.07 (s, 3H, NCH_3), 3.19 (s, 3H, NCH_3), 3.54 (ddd, 1H, CH_2, $^2J_{HH}$ = 15.9, $^2J_{HP}$ = 7.77), 3.93 (ddd, 1H, CH_2, $^2J_{HH}$ = 15.9, $^2J_{HP}$ = 7.77), 6.94 (ddd, 1H, Ar, $^3J_{HH}$ = 6.4, $^3J_{HP}$ = 8.0, $^4J_{HP}$ = 1.3), 7.01 (pt, 1H, Ar), 7.13 (pt, 1H, Ar), 7.24 (m, 4H, Ar), 7.41 (m, 4H, Ar), 7.53 (m, 4H, Ar), 8.18 (dd, 1H, Ar, $^3J_{HH}$ = 7.5, $^3J_{HP}$ = 14.2). $^{31}P\{^1H\}$ NMR: δ −23.0 (d, $^2J_{PP}$ = 21.9, $^2J_{PPt}$ = 260, *P*-Pd), −31.7 (d, $^2J_{PP}$ = 21.9, $^1J_{PPt}$ = 4200, *P*-Pt).

PdCl$_2$(dmpam), 3. To *trans*-$PdCl_2(PhCN)_2$ (31 mg, 0.081 mmol) and dmapm (48 mg, 0.086 mmol) was added CH_2Cl_2 (5 mL). After the solution was stirred for 5 min, the volume was reduced in vacuo to ~1 mL, and Et_2O (20 mL) was added to give a yellow powder that was collected, washed with Et_2O (3 × 3 mL), and dried under vacuum. Yield: 54 mg (92%). Anal. Calcd for $C_{33}H_{42}N_4Cl_2P_2Pd$: C, 54.0; H, 5.8; N, 7.6. Found: C, 53.8; H, 5.9; N, 7.4. UV−vis (CH_2Cl_2): 360 [3870]. Data follow for PdCl$_2$(*P*,*P*′-dmapm), **3a.** ^1H NMR: δ 2.35 (s, 24H, NCH_3), 5.31 (t, 2H, CH_2, $^2J_{HP}$ = 12.1). The aromatic ^1H signals of **3a** and **3b** overlap (δ 6.4−8.2) and could not be resolved. $^{31}P\{^1H\}$ NMR: δ −56.8 (s). Data follow for PdCl$_2$(*P*,*N*-dmapm), **3b.** ^1H NMR (240 K): δ 1.61 (s, 3H, NCH_3), 2.43 (s, 6H, NCH_3), 2.87 (pt, 1H, CH_2), 2.91 (s, 3H, NCH_3), 2.97 (s, 6H, NCH_3), 3.46 (s, 3H, NCH_3), 3.79 (s, 3H, NCH_3), 4.01 (pt, 1H, CH_2). $^{31}P\{^1H\}$ NMR (215 K): δ −39.8 (d, $^2J_{PP}$ = 88.9), 35.4 (d, $^2J_{PP}$ = 88.9). X-ray quality crystals of **3b** were grown by slow evaporation from a $CDCl_3$ solution.

PdBr$_2$(dmapm), 4. To **1** (77 mg, 0.10 mmol) and NaBr (170 mg, 1.7 mmol) were added acetone (10 mL) and H_2O (2 mL). The yellow slurry was stirred for 2 h before evaporation to dryness. The residue was taken up in CH_2Cl_2 (10 mL) and the mixture filtered through Celite 545. The filtrate volume was reduced in vacuo to ~1 mL, and Et_2O (20 mL) was added to give a yellow powder that was collected, washed with Et_2O (3 × 3 mL), and dried under vacuum. Yield: 55 mg (64%). Anal. Calcd for $C_{33}H_{42}N_4Br_2P_2Pd$: C, 48.2; H, 5.1; N, 6.8. Found: C, 48.1; H, 5.1; N, 6.6. UV−vis (CH_2Cl_2): 378 [4310]. Data follow for PdBr$_2$(*P*,*P*′-dmapm), **4a**. ^1H NMR (250 K): δ 2.30 (br s, 24H, NCH_3), 5.41 (t, 2H, CH_2, $^2J_{HP}$ = 12.0). The aromatic ^1H signals of the two isomers again overlap (δ 6.3−7.9). $^{31}P\{^1H\}$ NMR (250 K): δ −58.5 (s). Data follow for PdBr$_2$(*P*,*N*-dmapm), **4b**. ^1H NMR (250 K): δ 1.61 (br s, 3H, NCH_3), 2.45 (s, 6H, NCH_3), 2.92 (s, 9H, NCH_3), 3.01 (pt, 1H, CH_2), 3.51 (s, 3H, NCH_3), 3.82 (s, 3H, NCH_3), 3.97 (pt, 1H, CH_2). $^{31}P\{^1H\}$ NMR (250 K): δ −40.4 (d, $^2J_{PP}$ = 112), 33.3 (d, $^2J_{PP}$ = 112).

PdI$_2$(dmapm), 5. To *trans*-$PdCl_2(PhCN)_2$ (91 mg, 0.24 mmol), dmapm (130 mg, 0.23 mmol), and NaI (190 mg, 1.3 mmol) was added CH_2Cl_2 (5 mL), followed after 5 min by acetone (10 mL) which caused a rapid color change from yellow to deep orange. The slurry was stirred for 2 h at rt before reduction to dryness in vacuo. The workup was the same as that for **2**. Yield: 180 mg (83%). Anal. Calcd for $C_{33}H_{42}N_4I_2P_2Pd$: C, 43.2; H, 4.6; N, 6.1. Found: C, 43.4; H, 4.7; N, 6.0. UV−vis (CH_2Cl_2): 304 [16100], 430 [4010]. Data follow for PdI$_2$(*P*,*P*′-dmapm), **5a**. ^1H NMR (250 K): δ 2.26 (br s, 24H, NCH_3), 5.58 (t, 2H, CH_2, $^2J_{HP}$ = 12.4). The aromatic ^1H signals of **5a** and **5b** again overlap (δ 6.3−8.0). $^{31}P\{^1H\}$ NMR: δ −65.6 (s). Data follow for PdI$_2$(*P*,*N*-dmapm), **5b**. ^1H NMR (250 K): δ 1.55 (br s, 3H, NCH_3), 2.46 (s, 6H, NCH_3), 2.80 (br s, 3H, NCH_3), 2.88 (s, 6H, NCH_3), 3.22 (pt, 1H, CH_2), 3.55 (s, 3H, NCH_3), 3.84 (s, 3H, NCH_3), 3.93 (pt, 1H, CH_2). $^{31}P\{^1H\}$ NMR: δ −40.8 (d, $^2J_{PP}$ = 98), 27.3 (d, $^2J_{PP}$ = 98).

Pd(CN)$_2$(*P*,*N*-dmapm), 6b. To a yellow slurry of **1** (46 mg, 0.063 mmol) and KCN (8.3 mg, 0.013 mmol) in EtOH (5 mL) was added H_2O (2 mL), whereupon a colorless solution formed. The solvent was removed in vacuo after 10 min, and the residue was taken up in CH_2Cl_2 (10 mL); this was filtered through Celite 545/$MgSO_4$, and the filtrate was reduced to ~1 mL. Addition of Et_2O (10 mL) gave the product as a white powder that was isolated by filtration, washed with Et_2O (3 × 3 mL), and dried under vacuum. Yield: 24 mg (54%). Anal. Calcd for $C_{35}H_{42}N_6P_2Pd$: C, 58.8; H, 5.9; N, 11.8. Found: C, 58.9; H, 6.0; N, 11.5. ^1H NMR (233 K): δ 1.57 (s, 3H, NCH_3), 2.33 (s, 6H, NCH_3), 2.74 (s, 3H, NCH_3), 2.96 (s, 6H, NCH_3), 3.11 (pt, 1H, CH_2), 3.41 (s, 3H, NCH_3), 3.61 (pt, 1H, CH_2), 3.77 (s, 3H, NCH_3), 6.39 (pt, 1H, Ar), 6.66 (m, 2H, Ar), 6.96 (m, 3H, Ar), 7.15 (pt, 1H, Ar), 7.22 (pt, 1H, Ar), 6.39 (pt, 1H, Ar), 7.32 (m, 5H, Ar), 7.48 (m, 2H, Ar), 7.72 (pt, 1H, Ar). $^{31}P\{^1H\}$ NMR (233 K): δ 21.1 (d, $^2J_{PP}$ = 130), −41.6 (d, $^2J_{PP}$ = 130).

PtCl$_2$(*P*,*P*′-dmapm), 7. The synthesis was identical in principle to that of **3**. Thus, PtCl$_2$(cod) (58 mg, 0.15 mmol) and dmapm (86 mg, 0.16 mmol) gave 83 mg (66%) of an off-white powder. Anal. Calcd for $C_{33}H_{42}N_4Cl_2P_2Pt$: C, 48.2; H, 5.2; N, 6.8. Found: C, 48.5; H, 5.4; N, 6.7. ^1H NMR: δ 2.24 (s, 24H, NCH_3), 5.77 (t, 2H, CH_2, $^2J_{HP}$ = 12.9, $^3J_{HPt}$ = 60), 7.17 (pt, 4H, Ar), 7.25 (pd, 4H, Ar), 7.44 (pt, 4H, Ar), 7.17 (br m, 4H, Ar). $^{31}P\{^1H\}$ NMR: δ −65.6 (s, $^1J_{PPt}$ = 3084).

Pd$_2$Cl$_2$(μ-CO)$_2$(μ-*P*:*P*′-dmapm), 8. To a Schlenk tube containing **1** (31 mg, 0.037 mmol) was admitted CO (1 atm), followed by

Et_2O (10 mL) and CH_2Cl_2 (2 mL). The orange slurry on being stirred overnight became blue-purple. The solid was collected, washed with Et_2O, and dried in vacuo. Yield: 21 mg (64%). Anal. Calcd for $C_{35}H_{42}N_4Cl_2O_2P_2Pd_2$: C, 46.9; H, 4.7; N, 6.2. Found: C, 46.4; H, 4.8; N, 6.3. ^{1}H NMR (under 1 atm CO): δ 2.67 (t, 2H, CH_2, $^2J_{HP}$ = 12.0 Hz), 2.72 (s, 24H, NCH_3), 7.12 (m, 8H, Ar), 7.45 (m, 8H, Ar). ^{31}P{^{1}H} NMR (under 1 atm CO): δ 43.0 (s). IR (KBr pellet): ν_{CO}: 1798 [s].

PdCl(η^2-DEAD)(μ-*P*:*P*′,*N*-dmapm)PdCl·H_2O, 9·H_2O. To a CH_2Cl_2 (5 mL) solution of **1** (63 mg, 0.075 mmol) was added DEAD (0.020 mL, 0.13 mmol). Over 10 h, the solution changed from red to yellow, and some decomposition to Pd metal occurred. After filtration through Celite 545, the solution was reduced in vacuo to ∼1 mL, and Et_2O (20 mL) was added to give the product as a fine yellow precipitate that was collected, washed with Et_2O (3 × 3 mL), and dried under vacuum. Yield: 44 mg (58%). Anal. Calcd for $C_{41}H_{54}N_4Cl_2O_5P_2Pd_2$: C, 47.9; H, 5.3; N, 5.4. Found: C, 47.8; H, 5.4; N, 5.4. ^{1}H NMR (325 K): δ 1.47 (t, 6H, CH_2CH_3, $^3J_{HH}$ = 6.9), 1.78 (s, 2H, H_2O), 2.32 (s, 12H, NCH_3), 2.84 (s, 6H, NCH_3), 2.89 (s, 6H, NCH_3), 3.19 (dt, 1H, PCH_2P, $^2J_{HH}$ = $^2J_{HP}$ = 14.0), 3.70 (m, 5H, PCH_2P and CH_2CH$_3$), 6.90 (pt, 2H, Ar), 7.05 (m, 2H, Ar), 7.35 (m, 8H, Ar), 7.50 (pt, 2H, Ar), 8.55 (m, 2H, Ar). ^{31}P{^{1}H} NMR (325 K): δ 31.6 (s).

***rac*-[PdPtCl$_2$(μ-*N*,*P*:*P*′,*N*′-dmapm)(μ-SEt)][OTf], *rac*-10.** Excess EtSH (0.044, mL, 0.54 mmol) and 1 equiv of TfOH (0.005 mL, 0.054 mmol) were added to a solution containing **2** (50 mg, 0.059 mmol) in CH_2Cl_2 (5 mL). The solution was stirred for 24 h and filtered through Celite 545/$MgSO_4$. The volume of the red filtrate was reduced in vacuo to ∼1 mL, and Et_2O (20 mL) was added to give the yellow product that was collected, washed with Et_2O (3 × 3 mL), and dried in vacuo. Yield: 32 mg (51%). Anal. Calcd for $PdPtCl_2P_2N_4C_{36}H_{47}S_2O_3F_3$: C 38.0, H, 4.1, N 4.8. Found: C 37.8, H 4.1, N 4.8. ^{1}H NMR (CD_3OD): δ 1.01 (t, 3H, CH_3CH$_2$, $^2J_{HH}$ = 7.3), 2.15 (q, 2H, CH_2S), 2.20 (br s, 12 H, NCH_3), 2.47 (s, 3H, NCH_3), 3.43 (m, 1H, CH_2) 3.55 (s, 3H, NCH_3), 3.60 (s, 3H, NCH_3), 3.66 (s, 3H, NCH_3), 3.94 (m, 1H, CH_2), 7.24−8.08 (m, 16H, Ar). ^{31}P{^{1}H} NMR (CD_3OD): δ 23.4 (d, $^2J_{PP}$ = 43.2, $^1J_{PPt}$ = 3900, *P*-Pt), 48.9 (d, $^2J_{PP}$ = 43.2, $^2J_{PPt}$ = 260, *P*-Pd). ^{19}F{^{1}H} NMR (CD_3OD): δ −3.5 (s). Λ_M (MeOH): 84. MS: 991 [M$^+$]. Single crystals suitable for X-ray analysis were obtained by slow diffusion of Et_2O into a methanolic solution of the complex.

***rac*-[PdPtCl$_2$(μ-*N*,*P*:*P*′,*N*′-dmapm)(μ-S^{n}Pr)][OTf], *rac*-11.** The synthesis was performed in a manner similar to that for ***rac*-10**. Thus, an excess ^{n}PrSH (0.044, mL, 0.54 mmol) and 1 equiv of TfOH (0.005 mL, 0.054 mmol) and **2** (50 mg, 0.059 mmol) gave 40.9 mg (66%) of a yellow powder. ^{1}H NMR: δ 0.66 (t, 3H, CH_3CH$_2$, $^2J_{HH}$ = 7.3), 1.38 (sp, 2H, CH_2CH$_2$S), 2.12 (q, 2H, CH_2S), 2.22 (br s, 12 H, NCH_3), 2.91 (m, 2H, CH_2) 3.46 (s, 3H, NCH_3), 3.54 (s, 3H, NCH_3), 3.59 (s, 3H, NCH_3), 3.66 (s, 3H, NCH_3), 7.27 (pt, 1H, Ar), 7.44 (m, 4H, Ar), 7.60 (pt, 2H, Ar), 7.74 (m, 4H, Ar), 8.03 (m, 4H, Ar), 8.26 (dd, 1H Ar, $^3J_{HH}$ = 9.5, $^3J_{HP}$ = 12.2). ^{31}P{^{1}H} NMR (CD_3OD): δ 23.1 (d, $^2J_{PP}$ = 43.0, $^1J_{PPt}$ = 3940, *P*-Pt), 48.6 (d, $^2J_{PP}$ = 43.5, $^2J_{PPt}$ = 300, *P*-Pd). ^{19}F{^{1}H} NMR (CD_3OD): δ −3.5 (s). MS: 1003 [M$^+$].

X-ray Crystallographic Analyses. Measurements were made at 173(1) K on a Rigaku/ADSC CCD area detector with graphite monochromated Mo Kα radiation (0.71069 Å). Some crystallographic data for **3b** and *rac*-**10** are shown in Table 1. The final unit cell parameters were based on 24451 reflections for **3b** and 21322 reflections for *rac*-**10** with 2θ = 4.1−55.8°. The data were collected and processed using the d*TREK program,[29] and the structures were solved using direct (for **3b**) or heavy-atom Patterson (for *rac*-**10**) methods,[30] and expanded using Fourier techniques.[31]

Table 1. Crystallographic Data for **3b** and *rac*-**10**

	3b	*rac*-**10**
formula	$C_{33}H_{42}N_4Cl_2P_2Pd$	$C_{36}H_{47}N_4Cl_2F_3O_3P_2PdPtS_2$
fw	733.98	1139.25
cryst color, habit	yellow, block	yellow, platelet
cryst size (mm^3)	0.30 × 0.15 × 0.15	0.30 × 0.15 × 0.03
space group	$P2_1/n$ (No. 14)	$C2/c$ (No. 15)
a (Å)	11.6675(4)	39.621(2)
b (Å)	19.8387(6)	11.7466(5)
c (Å)	14.9924(7)	17.8781(8)
β (deg)	99.291(3)	89.228(3)
V (Å^3)	3424.7(2)	8320.0(6)
μ (cm^{-1})	8.20	41.38
total reflns	29535	38644
unique reflns	7350	9662
R_{int}	0.055	0.067
no. variables	379	489
R1 ($I > 3\sigma(I)$)[a]	0.027 (5198 observns)	0.030 (5755 observns)
wR2[b]	0.080	0.076
GOF	0.86	0.93

[a] $R1 = \sum||F_o| - |F_c||/\sum|F_o|$ (observed data). [b] $wR2 = [\sum(F_o^2 - F_c^2)^2/\sum w(F_o^2)^2]^{1/2}$ (all data).

Scheme 2. Solution Equilibrium Behavior of $PdCl_2$(dmapm) in $CDCl_3$

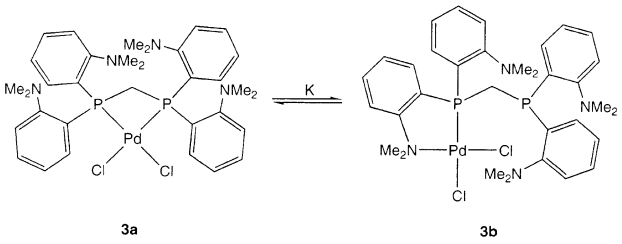

3a 3b

The non-hydrogen atoms were refined anisotropically, and the H atoms were included but not refined. In *rac*-**10**, there was some disorder at both metal atoms: the electron density at Pd was greater than expected (but less than for one Pt), and at Pt was less than expected (but greater than for one Pd), so the populations at Pd and Pt were refined with values of 0.82 and 1.28, respectively, to fit better the total electron density at each site.

Results and Discussion

Solution Behavior and Structure of Monometallic Complexes. The isolated product **3** from the 1:1 reaction between dmapm and *trans*-$PdCl_2(PhCN)_2$ exists in $CDCl_3$ as a mixture of $PdCl_2$(*P*,*P*′-dmapm) (**3a**) and $PdCl_2$(*P*,*N*-dmapm) (**3b**) that show, respectively, a singlet and an AB doublet of doublets in their ^{31}P{^{1}H} NMR spectra (see Experimental Section). Varying the temperature reversibly alters the relative peak intensities, showing that **3a** and **3b** are in thermal equilibrium (Scheme 2); **3b** becomes increasingly dominant at lower temperatures.

(29) *d*TREK: Area Detector Software*; Molecular Structure Corporation: The Woodlands, TX, 1997.

(30) (a) Altomare, A.; Burla. M. C.; Cammalli, G.; Cascarano, M.; Giacovazzo, C.; Guagliardi, A.; Moliterni, A. G. G.; Polidori, G.; Spagna, A. *J. Appl. Crystallogr.* **1999**, *32*, 115. (b) Beurskens, P. T.; Admiraal, G.; Beurskens, G.; Bosman, W. P.; Garcia-Granda. S.; Gould, R. O.; Smits, J. M. M.; Smykalla, C. *The DIRDIF-PATTY-Program System*; Technical Report of the Crystallography Laboratory; University of Nijmegen: Nijmegen, The Netherlands, 1992.

(31) Beurskens, P. T.; Admiraal, G.; Beurskens, G.; Bosman, W. P.; de Gelder, R.; Israel, R.; Smits, J. M. M. *The DIRDIF-94 Program System*; Technical Report of the Crystallography Laboratory; University of Nijmegen: Nijmegen, The Netherlands, 1994.

In contrast to the linkage isomerism of **3**, the Pt analogue, made from $PtCl_2$(cod) and dmapm, exists solely as $PtCl_2$-(*P*,*P*′-dmapm) (**7**). The thermodynamic stability of **7** has important ramifications for the reactivity of mixed-metal complex **2** (vide infra).

The number and relative integrations of the ^{1}H NMR singlets due to the NCH_3 protons of dmapm complexes are informative about their molecular structures (for free dmapm, this signal appears at δ 2.68). In the ^{1}H NMR spectrum (300 K) of **3**, five singlets due to NCH_3 protons are seen at δ 3.70, 3.47, 2.85, 2.49, and 2.35 with relative integrations of 1:1:2:2:3, respectively. These represent all 24 NMe protons associated with **3a** (δ 2.35) and 18 of the 24 corresponding protons of **3b**. The remaining 6 NMe protons of **3b** give signals that are broadened into the baseline. At 240 K, these "missing" protons appear as singlets at δ 1.61 and 2.91, while the peak due to **3a** diminishes (see Supporting Information (SI), Figure S1.) The two new peaks likely correspond to the two Me groups on the free anilinyl ring associated with the Pd-bound P-atom. In the solid-state structure of **3b** (vide infra), the N(2)-atom of this ring is oriented towards the Pd center with which it shows a close contact (3.32 Å; the sum of the van der Waals radii of Pd and N = 3.18 Å). The broadened peaks at 300 K likely result from the rapid, reversible coordination of this anilinyl ring.

From the relative intensities of the peaks at δ 2.35 and 3.70 (which shift marginally downfield with decreasing temperature), equilibrium constants (*K*'s) for the **3a**,**b** isomerization from 215 to 300 K have been calculated, and the corresponding van't Hoff plot yielded $\Delta H° = -5.5 \pm 0.5$ kJ mol^{-1} and $\Delta S° = -10 \pm 1$ J K^{-1} mol^{-1} (see SI, Figure S2.). Thermochemical data for the substitution of the PhCN of *trans*-$PdCl_2(PhCN)_2$ by PPh_3 and pyridine (py) have shown previously that the Pd−PPh_3 bond is stronger than the Pd−py bond by 27 kJ mol^{-1},[32] and we have used this value for the energy difference between the Pd−P bond in **3a** and the Pd−N bond in **3b**. If $\Delta H°$ for the **3a**,**b** equilibrium is assumed to be the sum of the enthalpic penalty for breaking the Pd−P bond and the combined gain from the formation of the Pd−N bond and alleviation of the four-membered ring strain, and, if the five-membered *P*,*N* ring in **3b** is assumed to be strain-free, then the four-membered ring strain energy in **3a** can be estimated to be ~32 kJ mol^{-1}. The ring strain energy values associated with the binding of chelated dppm to "(C_5R_5)RuCl" (R = H, Me), estimated by comparison of the heats of reaction for the substitution of cod by dppm and PPh_2Me in (C_5R_5)Ru(cod)Cl, are 42 and 56 kJ mol^{-1} for R = H and R = Me, respectively.[33,34] Our lower value is consistent with weaker Pd−P bonding relative to that of Ru−P.

Bromo (**4**) and iodo (**5**) complexes are readily made by reaction of **3** with excess NaX (X = Br, I), and these also exist in $CDCl_3$ as equilibrium mixtures of the *P*,*P*′- and *P*,*N*-isomers. The **a**,**b** equilibrium constants at 250 K for **3**, **4**, and **5** are 4.1, 4.8, and 6.3, respectively. Pringle and Shaw discovered that $PdCl_2$(*P*,*P*′-dppm) reacts with NaCN to give the face-to-face species [*trans*-$Pd(CN)_2$(μ-*P*:*P*′-dppm)]$_2$.[35] In contrast, **3** reacts with 2 equiv of KCN to give exclusively $Pd(CN)_2$(*P*,*N*-dmapm) (**6b**); **6a** is not detected at 215 K, implying that $K > 100$ for the **6a**,**b** equilibrium. Thus, the magnitudes of *K* for the **a**,**b** equilibria correlate with the position of X in the trans effect series (Cl < Br < I ≪ CN);[36] as P-donors also show a strong trans effect, PdX_2(*P*,*N*-dmapm) (**b**) should be progressively more stable than PdX_2-(*P*,*P*′-dmapm) (**a**) as the trans effect of X increases.

The crystal structure of **3b** is shown in Figure 1, and relevant bond distances and angles are given in Table 2. Of importance, the structure allows for a direct comparison between both bound and free N- and P-atoms of identical type in the same molecule and, thus, permits an assessment of the relative degrees of σ- and π-bonding between these atoms and the metal. The variations in P−C bond lengths on coordination of dmapm to Pd(II) can be rationalized in light of the hypothesis, supported by calculations by Marynick[37] and Xiao et al.,[38] that P-based π-acceptor orbitals

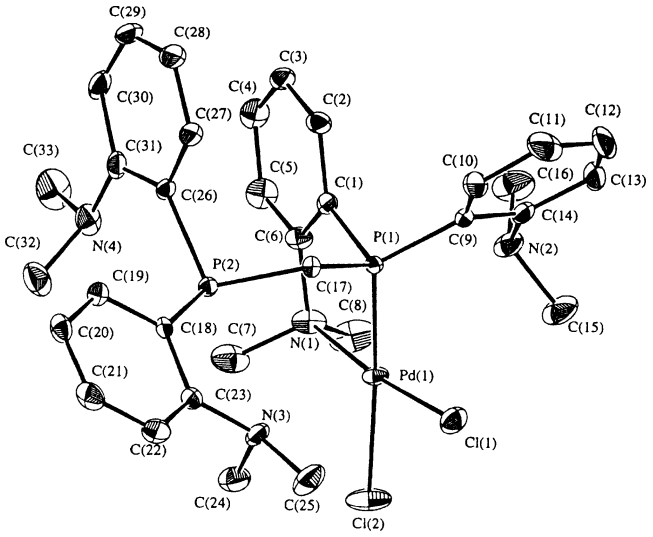

Figure 1. ORTEP diagram of **3b**, with 50% probability ellipsoids.

Table 2. Selected Bond Lengths (Å) and Angles (deg) for **3b**

Pd(1)−P(1)	2.1798(6)	P(2)−C(18)	1.847(2)
Pd(1)−N(1)	2.132(2)	P(2)−C(26)	1.845(2)
Pd(1)−Cl(1)	2.3041(6)	N(1)−C(6)	1.481(3)
Pd(1)−Cl(2)	2.3812(6)	N(1)−C(7)	1.492(4)
P(1)−C(1)	1.801(2)	N(1)−C(8)	1.490(3)
P(1)−C(9)	1.806(2)	N(3)−C(23)	1.425(3)
P(1)−C(17)	1.824(2)	N(3)−C(24)	1.467(3)
P(2)−C(17)	1.873(2)	N(3)−C(25)	1.453(3)

P(1)−Pd(1)−N(1)	86.10(6)	P(1)−Pd(1)−Cl(1)	87.93(2)
Cl(1)−Pd(1)−Cl(2)	92.63(2)	N(1)−Pd(1)−Cl(2)	93.54(6)
P(1)−C(17)−P(2)	108.4(1)	C−P(1)−C	107.4 (av)
C−P(2)−C	100.5 (av)		

(32) Partenheimer, W.; Hoy, E. F. *Inorg. Chem.* **1973**, *12*, 2805.
(33) Luo, L.; Zhu, N.; Zhu, N.-J.; Stevens, E. D.; Nolan, S. P.; Fagan, P. J. *Organometallics* **1994**, *13*, 669.
(34) Li, C.; Cucullu, M. E.; McIntyre, R. A.; Stevens, E. D.; Nolan, S. P. *Organometallics* **1994**, *13*, 3621.
(35) Pringle, P. G.; Shaw, B. L. *J. Chem. Soc., Chem. Commun.* **1982**, 956.
(36) Appleton, T. G.; Clark, H. C.; Manzer, L. E. *Coord. Chem. Rev.* **1973**, *10*, 335.
(37) Marynick, D. S. *J. Am. Chem. Soc.* **1984**, *106*, 4064.
(38) Xiao, S.-X.; Trogler, W. C.; Ellis, D. E.; Berkovich-Yellin, Z. *J. Am. Chem. Soc.* **1983**, *105*, 5.

(the LUMOs) are not purely 3d but have significant 3p character and local σ^* symmetry with respect to the P−C bonds. In addition, Orpen and Connelly propose that when the potential for π-back-bonding exists, a phosphine ligand responds to give a lower overall energy by adopting a more pyramidal geometry, enabling better overlap between the P 3d and P−C σ^* orbitals that together constitute the π-acceptor LUMOs.[39] This leads to a compression of the C−P−C angles and a lengthening of the P−C bonds. Conversely, when a phosphine acts predominantly as a σ-donor, the ligand adopts a more trigonal planar geometry with larger C−P−C angles giving better overlap for P−C σ-bonding and shorter P−C bonds. This latter case is observed in the solid-state structure of **3b**: the P−C bond lengths involving the bound P(1)-atom, both for P−C(aromatic) (av 1.804 Å) and P−C(aliphatic) (1.824 Å), are significantly shorter than those involving the free P(2)-atom (av 1.846 and 1.873 Å, respectively); in addition, the angles surrounding P(1) average 107.4°, larger than those found at P(2) (av 100.5 °). It is thus reasonable to rationalize the Pd−P bonding in **3b** in terms of a dominant P→Pd σ-contribution; this conforms to the observation that the relative importance of π- with respect to σ-bonding decreases on going from left to right across the transition series (as metal d-electrons become increasingly tightly bound).[40] In addition, the N−C bonds at the bound N-atom, N−C(aromatic) (1.481 Å) and N−C(aliphatic) (av 1.491 Å), are longer than those involving the free N-atoms (av 1.430 and 1.463 Å, respectively). As nitrogen has no d-orbitals available for bonding, the observed increase in N−C bond lengths upon coordination suggests that the so-called N-based "sp^3 nonbonding lone pair" has some N−C σ-character; depopulation of this orbital on coordination would induce a lengthening of the N−C bonds.

The Pd(1)−Cl(1) bond of **3b** is shorter than the Pd(1)−Cl(2) bond because of the higher trans influence of P with respect to N.[36] The Pd(1)−P(1) bond (2.1798 Å) is unusually short, as judged by the mean Pd−P distances for PMe_3, PPh_3, $PPhMe_2$, dppe, and dppm complexes of 2.287, 2.308, 2.253, 2.260, and 2.258 Å, respectively, calculated by Orpen et al.[41] The P(1)−C(17)−P(2) angle of 107.4 ° is intermediate between the compressed P−C−P angles found in four-membered *P*,*P*′-metallacycles (e.g., 93.0° for $PdCl_2$(dppm)[42]) and those found in complexes containing η^1-dppm (e.g., 118.9° for *trans*-Ru(η^1-dppm)$_2$(*N*,*O*-quin)$_2$; quin = 2-quinaldinate anion[43]). The P(1)−Pd(1)−N(1) "bite" angle is 86.1°, similar to those found in Ru(II) complexes of 2-(diphenylphosphino)-*N*,*N*-dimethylaniline, which are 80−83° within both five- and six-coordinate complexes.[44]

Synthesis and Reactivity of Bimetallic Complexes. Our recently reported, structurally characterized Pd_2Cl_2(μ-*N*,P:*P*′,*N*′-dmapm) complex (**1**), containing dmapm in a *P*,*P*′-bridging-bis(*P*,*N*)-chelating coordination mode, was made by the conproportionation reaction of **3** and $Pd_2(dba)_3$ (dba = dibenzylideneacetone).[25] Although several reducing agents have been used in attempted syntheses of group 10, M^I-M^I bonded complexes,[45] the conproportionation route involving M^{II} and M^0 complexes in the presence of a bridging ligand tends to give the best results.[46] The mixed-metal complex $PtPdCl_2$(μ-*P*:*P*′-dppm)$_2$ was first made by such a route using in situ $PtCl_2(NC^tBu)_2$/dppm and $Pd(PPh_3)_4$/dppm systems as precursors,[47] and corresponding complexes containing bridging 2-pyridylphosphine ligands have been made similarly.[48] However, our attempts to make $PtPdCl_2$(μ-*N*,*P*:*P*′,*N*′-dmapm) (**2**) from **3** and Pt(dba)$_2$ were unsuccessful; **2** was made instead via the 2-electron reduction of in situ formed $PtPdCl_4$-(μ-*N*,*P*:*P*′,*N*′-dmapm)[26] by hot ethanolic KOH. Reduction of Pt^{II} salts by ethanolic KOH is well-known (e.g., in the synthesis of $Pt(PPh_3)_4$ from K_2PtCl_4),[49] but to our knowledge, the synthesis of **2** represents the first time that the method has been used to make a M^I-M^I complex from the corresponding M^{II}_2 compound.

The $^{31}P\{^1H\}$ data for **2** reveal inequivalent P-atoms, the higher field resonance showing ^1J coupling to Pt, while the P-atom at the Pd shows ^2J coupling to Pt. The NMe groups are manifest as 6 singlets in the ^1H NMR with relative intensities of 2:2:1:1:1:1. By virtue of their similar positions in the spectrum of **1**,[25] the singlets at δ 3.07 and 2.78, and 2.45 are assigned to the 2 diastereotopic NMe groups of the Pd-bound N-atom and the 2 equivalent NMe groups of the free N-atom associated with the Pd-bound P-atom, respectively. The remaining peaks at δ 3.19, 3.02, and 2.36 correspond to the analogous NMe protons on the "Pt-side" of the molecule.

Exposure of an orange $CDCl_3$ solution of **1** to 1 atm of CO resulted in a rapid color change to intense purple. The in situ $^{31}P\{^1H\}$ NMR spectrum showed a singlet at δ_P 43.0 for the product (**8**), and the δ_P −29.9 singlet of unreacted **1**, in a ratio of ∼6:1. The ^1H NMR spectrum showed that all 24 NMe protons of **8** were equivalent, implying that the coordinated N-atoms of **1** had been displaced by CO. Conducting three freeze−pump−thaw cycles on the product solution regenerated **1** quantitatively. The isolated, purple solid **8** revealed a single, strong IR band at 1798 cm^{-1}, attributed to μ-CO, and analyzed correctly for $Pd_2Cl_2(CO)_2$-(dmapm). Its proposed structure (Scheme 3) contains a μ-*P*:*P*′-dmapm ligand, and bridged CO ligands on both sides of a Pd−Pd bond that maintain a 16 e^- requirement. The ν_{sym}(CO) would be IR-invisible. The CO reaction has analogies to that of Pd_2Cl_2[μ-*P*:*N*-PPh_2(2-pyridyl)]$_2$, but here, the pyridyl N-donors are replaced by terminal CO ligands (ν_{CO}: 1994, 2019 cm^{-1}).[50] In contrast, Pd_2Cl_2(μ-*P*,*P*′-dppm)$_2$

(39) Orpen, A. G.; Connelly, N. G. *Organometallics* **1990**, *9*, 1206.
(40) Dunne, B. J.; Morris, R. B.; Orpen, A. G. *J. Chem. Soc., Dalton Trans.* **1991**, 653.
(41) Orpen, A. G.; Brammer, L.; Allen, F. H.; Kennard, O.; Watson, D. G. *J. Chem. Soc., Dalton Trans.* **1989**, S1.
(42) Steffen, W. L.; Palenik, G. J. *Inorg. Chem.* **1976**, *15*, 2432.
(43) Barral, M. C.; Jiménez-Aparicio, R.; Royer, E. C.; Saucedo, M. J.; Urbanos, F. A. *Inorg. Chim. Acta* **1993**, *209*, 105.
(44) Mudalige, D. C.; Ma, E. S.; Rettig, S. J.; James, B. R.; Cullen, W. R. *Inorg. Chem.* **1997**, *36*, 5426.
(45) Pringle, P. G.; Shaw, B. L. *J. Chem. Soc., Dalton Trans.* **1983**, 889.
(46) Balch, A. L.; Benner, L. S. *Inorg. Synth.* **1982**, *21*, 47.
(47) Pringle, P. G.; Shaw, B. L. *J. Chem. Soc., Chem. Commun.* **1982**, 81.
(48) Xie, Y.; Lee, C.-L.; Yang, Y. P.; Rettig, S. J.; James, B. R. *Inorg. Chim. Acta* **1994**, *217*, 209.
(49) Ugo, R.; Cariati, F.; Monica, G. L. *Inorg. Synth.* **1968**, *11*, 105.
(50) Maisonnat, A.; Farr, J. P.; Balch, A. L. *Inorg. Chim. Acta* **1981**, *53*, L217.

Scheme 3. Reversible Reaction of **1** with CO to Give **8**

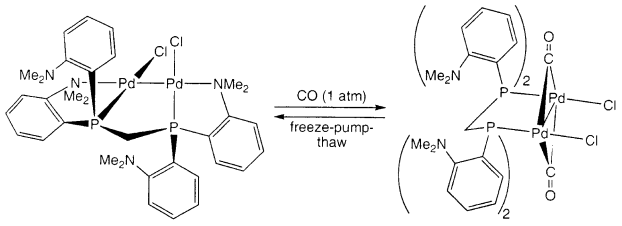

Scheme 4. Proposed Fluxionality of Complex **9** (R = CO_2Et)

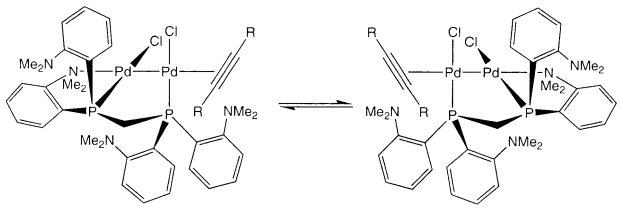

reversibly binds 1 equiv of CO to give the "A-frame" product $Pd_2Cl_2(\mu\text{-CO})(\mu\text{-}P,P'\text{-dppm})_2$ (ν_{CO}: 1705 cm^{-1}).[51]

Complex **1** also reacted with the electron deficient alkyne, DEAD, to give a product (**9**) of formula Pd_2Cl_2(DEAD)-(dmapm). At 325 K, the $^{31}P\{^1H\}$ NMR spectrum in $CDCl_3$ shows just a slightly broadened singlet (δ_P 31.6) that at 220 K becomes two doublets (δ_P 19.3 and 44.3; $^2J_{PP}$ = 68 Hz) (SI, Figure S3). One possible interpretation is illustrated in Scheme 4 (R = CO_2Et), where reversible coordination of an N-atom causes the acetylene to shuttle between the Pd atoms, the two species in equilibrium being enantiomers of PdCl(η^2-DEAD)(μ-*P*:*P*′,*N*-dmapm)PdCl (**9**). In a "frozen" state at low temperature, the two P-atoms become inequivalent, while at higher temperatures, the P-atoms are rendered equivalent by rapid exchange. More typically, acetylenes react with Pd^I_2-complexes to generate species in which the unsaturated ligand acts as a μ-η^1:η^1 donor lying parallel to the Pd−Pd axis;[52] such a structure, i.e., $Pd_2Cl_2(\mu\text{-}\eta^1\text{:}\eta^1$-DEAD)($\mu$-*N*,*P*:*N*′,*P*′-dmapm), would provide an appropriate transition state for the shuttling mechanism. A 2D ^{31}P EXSY measurement at 220 K confirmed that the P-atoms of **9** are indeed in chemical exchange. The Me groups appear in the ^1H NMR at 325 K as 3 singlets with relative integrations 1:1:2, corresponding to 2 diastereotopic sets of Me groups on the Pd-bound N-atoms, and one set of equivalent Me groups of the free N-atoms.[25]

In contrast to the reactions of CO and DEAD with **1**, which gave the stable products **8** and **9**, analogous reactions with **2** at rt resulted in disproportionation of **2** to Pd metal and $PtCl_2$(*P*,*P*′-dmapm) (**7**). At 233 K, however, $^{31}P\{^1H\}$ data revealed the presence of two intermediates in the CO reaction, although the corresponding ^1H spectra revealed only broad and uninformative resonances. Data for the first observed intermediate **I** were the following: δ_P −18.4 (d, $^1J_{PPt}$ = 3060, $^2J_{PP}$ = 23.3 Hz, *P*-Pt), −8.3 (d, $^2J_{PPt}$ = 300, $^2J_{PP}$ = 23.3 Hz, *P*-Pd). The observation of the $^2J_{PPt}$ coupling requires that the Pd−Pt bond remains intact (cf. the $^{31}P\{^1H\}$ data for **2**, where $^2J_{PPt}$ =260 Hz, and the fact that

Chart 3. Possible Structure of Intermediate **I**

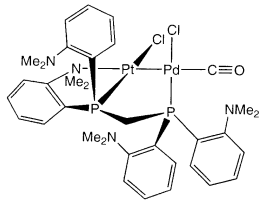

no $^2J_{PPt}$ coupling is observed for the non-metal−metal bonded, $Pt^{II}Pd^{II}$ complex shown in Chart 2 [26]), thus likely ruling out a species with a single bridged CO. Initial substitution of one N-atom donor by a terminal CO gives the most reasonable formulation for **I** (Chart 3); substitution at the more labile Pd atom is shown, but similar reactivity at the Pt cannot be ruled out (a Pt−CO bond is more stable than a corresponding Pd−CO bond).[53] For intermediate **II**, data were the following: δ_P 25.6 (d, $^1J_{PPt}$ = 5120, $^2J_{PP}$ = 173 Hz, *P*-Pt), 46.9 (d, $^2J_{PPt}$ = 1270, $^2J_{PP}$ = 173 Hz, *P*-Pd); the large downfield shifts of peaks relative to shifts of **2** (δ_P −31.7 and −23.0) are comparable to that for **8** (δ_P 43.0) relative to that of **1** (δ_P −29.9), and a structure such as **8** with two bridging carbonyls (Scheme 3), but with mixed metals, seems feasible for **II**. That the downfield shifts for **I** are much smaller than those of **II** (vs shifts for **2**) perhaps supports a less dramatic structural change in forming **I** versus **II**. Intermediates **I** and **II** appeared after ∼30 min at 233 K and increased in concentration as **2** was consumed; at 263 K, **7** (δ_P −65.2) appeared and at 300 K was the sole P-containing product. It is not obvious how reaction of **2** with CO (or DEAD) leads to disproportionation to Pd^0 and Pt^{II}; the incoming unsaturated ligand clearly promotes electron transfer between the Pd^I and Pt^I states via (in the CO system) intermediates such as **I** or **II**.

The reaction of **2** and thiols (RSH) in the presence of triflic acid (HOTf) generated the bridged-thiolate complexes *rac*-[PtPd(μ-SR)(μ-*N*,*P*:*P*′,*N*′-dmapm)][OTf] (R = Et (*rac*-**10**), ^{n}Pr (*rac*-**11**)) and H_2 (Scheme 1, M = Pt); we have reported recently[25] on the corrresponding reaction of the homobimetallic complex **1** and ^{n}PrSH (including its mechanism) that gave *rac*-[Pd_2(μ-S^{n}Pr)(μ-*N*,*P*:*P*′,*N*′-dmapm)][OTf] (*rac*-**12**). The molecular structure of *rac*-**10** (Figure 2, with selected bond lengths and angles in Table 3) is very similar to that of *rac*-**12**, although the P(1)−C(17)−P(2) angle in this (115.6(3)°) is slightly more open than in the homobimetallic case (112.9(1)°). *rac*-**10** consists of two corner-sharing square planes that are not in the typical "A"-frame orientation because of the constraint imposed by the chirality of the P-atoms that, in Figure 2, both have *S* absolute configuration (the *C*2/*c* space group necessitates that the *R*,*R*-enantiomer is also present in equal abundance in the unit cell). In classical "A"-frame complexes such as $Pd_2Cl_2(\mu\text{-S})(\mu\text{-}P\text{:}P'$-dppm)$_2$, the P−Pd−P axes are approximately parallel, and both P-atoms of each dppm ligand are on the same side of the plane defined by the Pd- and S-atoms.[54] The analogous P−Pd−Cl and P−Pt−Cl axes in *rac*-**10** cannot be parallel

(51) Benner, L. S.; Balch, A. L. *J. Am. Chem. Soc.* **1978**, *100*, 6099.
(52) Xie, L. Y.; James, B. R. *Inorg. Chim. Acta* **1994**, *217*, 209.
(53) Calderazzo, F.; Dell'Amico, D. B. *Pure Appl. Chem*. **1986**, *58*, 56.
(54) James, B. R. *Pure Appl. Chem.* **1997**, *69*, 2213.

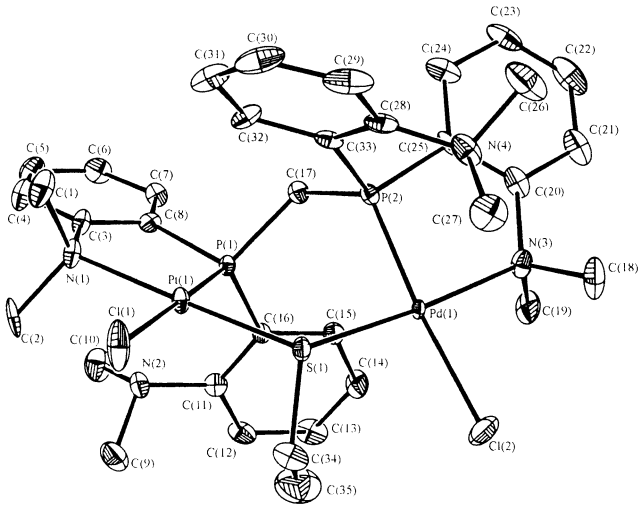

Figure 2. ORTEP diagram of the cation of *rac*-**10**, with 50% probability ellipsoids.

Table 3. Selected Bond Distances (Å) and Angles (deg) for *rac*-**10**

Pd(1)−S(1)	2.288(1)	Pt(1)−S(1)	2.306(1)
Pd(1)−P(2)	2.186(1)	Pt(1)−P(1)	2.189(1)
Pd(1)−Cl(2)	2.370(1)	Pt(1)−Cl(1)	2.377(1)
Pd(1)−N(3)	2.164(2)	Pt(1)−N(1)	2.162(4)
Pd(1)−S(1)−Pt(1)	121.61(5)	P(1)−C(17)−P(2)	115.6(3)
P(2)−Pd(1)−N(3)	85.0(1)	P(1)−Pt(1)−N(1)	85.9(1)
P(2)−Pd(1)−S(1)	91.01(5)	P(1)−Pt(1)−S(1)	96.55(5)
P(2)−Pd(1)−Cl(2)	173.76(6)	P(1)−Pt(1)−Cl(1)	177.28(5)
N(3)−Pd(1)−S(1)	174.5(1)	N(1)−Pt(1)−S(1)	176.6(1)

because the Cl-atoms fall on either side of the plane defined by the metal- and S-atoms as a result of the P-atoms having the same configuration. A putative *meso*-**10** could attain a classical "A"-frame structure. The solution $^{31}P\{^{1}H\}$ NMR spectrum of the isolated **10**, or of an in situ reaction mixture of **2** and EtSH (which is similar to that of **2**, but shifted downfield), showed no evidence for diastereomers (i.e., no doubling of the resonances), and thus, *rac*-**10** must be formed diastereoselectively. This is presumably because the precursor **2** is also formed diastereoselectively (i.e., the N-atoms do not exchange, or exchange only in a concerted manner), during the reaction of **2** and EtSH. Identical findings were seen for formation of *rac*-**12** from **1**.[25] The sets of ^{1}H NMR signals seen for the NMe protons of **10** and **11** are similar to those seen for **2**, although the 2 sets for the free N-atoms overlap to give a broad signal integrating for 12 protons.

Stereochemical considerations are pertinent for bimetallic catalysts. In hydroformylations catalyzed by Stanley's dirhodium complexes, which are based on the ligand $R_2P(CH_2)_2PR'CH_2PR'(CH_2)_2PR_2$ (R = Et, R′ = Ph), the *rac*-form is much more active than the *meso*-form.[20] Anderson and coworkers have recently reported Pt^{II}_2 and Pd^{II}_2 complexes containing a related tetraphosphine ligand (R = R′ = Ph).[55] Both tetraphosphine systems required physical separation of the two diastereomers. With the dmapm-bridged metal−metal bonded species, however, the *rac*-diastereomer is formed selectively, and no separation is necessary. In addition, the diastereoselection appears to be fixed at this stage and is conserved in subsequent reaction with thiols (and perhaps other small molecules). The preferred *rac*-coordination (vs *meso*) within the tetraphosphine systems has also been noted.[56]

Conclusions

The dmapm ligand is a versatile scaffold for the synthesis of metal−metal bonded homobimetallic (Pd_2) and heterobimetallic (PtPd) complexes in which it adopts a *P*,*P*′-bridging-bis(*P*,*N*-chelating) coordination mode. Only the *rac*-$MPdCl_2$-(μ-*N*,*P*:*P*′,*N*′-dmapm) diastereomer is formed, and this selectivity is conserved on reaction of these with thiols. This preference may make metal catalysts based on dmapm more attractive than those based on P_4-donors, which require separation of *meso* and *rac* forms. Hopefully, systems can be found that circumvent the problem of fragmentation of the catalyst.[20,26]

Reactions of small molecules with bis(P−P)-bridged bimetallic complexes are characterized by single insertions into the metal−metal bonds. By contrast, *rac*-Pd_2Cl_2(μ-*N*,*P*:*P*′,*N*′-dmapm) gives not only such insertion products (e.g., with RSH), but also doubly bridged adducts (e.g., with CO), and fluxional species involving exchange of bound and free anilinyl rings (e.g., with DEAD). Again, the extended range of coordination modes available to dmapm-bridged complexes may make them more useful as catalysts than those based on P−P-type ligands.

Acknowledgment. We thank the Natural Sciences and Engineering Council of Canada for financial support and the University of British Columbia for a University Graduate Fellowship (N.D.J.).

Supporting Information Available: X-ray crystallographic data for the structures of the **3b** and *rac*-**10** in CIF format. Variable temperature ^{1}H NMR spectra of an equilibrium mixture of **3a** and **3b** (Figure S1), the van't Hoff plot for this equilibrium (Figure S2), and $^{31}P\{^{1}H\}$ NMR spectra for **9** at 325 and 220 K (Figure S3). This information is available free of charge via the Internet at http://pubs.acs.org.

IC040019T

(55) Nair, P.; Anderson, G. K.; Rath, N. P. *Inorg. Chem. Commun.* **2002**, *5*, 653.
(56) (a) Aubry, D. A.; Laneman, S. A.; Fronczek, F. R.; Stanley, G. G. *Inorg. Chem.* **2001**, *40*, 5036. (b) Hunt, C. H.; Fronczek, F. R.; Billodeaux, D. R.; Stanley, G. G. *Inorg. Chem.* **2001**, *40*, 5192.